Environ. Sci. Technol. **2005**, *39,* 5481−5487

Arsenic Leachability in Water Treatment Adsorbents

CHUANYONG JING,*,† SUQIN LIU,†
MANISH PATEL,‡ AND
XIAOGUANG MENG†

Center for Environmental Systems, Stevens Institute of Technology, Hoboken, New Jersey 07030, and New Jersey Department of Environmental Protection, P.O. Box 409, Trenton, NJ 08625.

Arsenic leachability in water treatment adsorbents was studied using batch leaching tests, surface complexation modeling and extended X-ray absorption fine structure (EXAFS) spectroscopy. Spent adsorbents were collected from five pilot-scale filters that were tested for removal of arsenic from groundwater in Southern New Jersey. The spent media included granular ferric hydroxide (GFH), granular ferric oxide, titanium dioxide, activated alumina, and modified activated alumina. The As leachability determined with the Toxicity Characteristic Leaching Procedure (TCLP, 0.1 M acetate solution) was below 180 μg L^{-1} for all spent media. The leachate As concentration in the California Waste Extraction Test (0.2 M citrate solution) was more than 10 times higher than that in the TCLP and reached as high as 6650 μg L^{-1} in the spent GFH sample. The EXAFS results indicate that As forms inner-sphere bidentate binuclear surface complexes on all five adsorbent surfaces. The As adsorption/desorption behaviors in each media were described with the charge distribution multisite complexation model. This study improved the understanding of As bonding structures on adsorptive media surfaces and As leaching behavior for different adsorbents.

Introduction

The U.S. Environmental Protection Agency (EPA) has adopted an arsenic maximum contaminant level (MCL) of 10 μg L^{-1}. The state of New Jersey has recently proposed an arsenic standard for drinking water of 5 μg L^{-1} (*1*). The more stringent arsenic drinking water standard requires the installation of new water treatment systems and upgrading of existing ones. Filtration treatment of arsenic in water using adsorbents is especially suitable for small community systems and individual homes because the filters do not require much effort to operate (*2*, *3*). Activated alumina adsorbent has been used commonly for removal of arsenic and fluoride. Recently, more effective adsorbent media, such as granular ferric hydroxide (GFH), granular ferric oxide (GFO), granular titanium dioxide (TiO$_2$), and modified activated alumina (MAA), have been developed for arsenic removal. As a result of the enhanced removal efficiency, large amounts of spent media with elevated arsenic content will be generated. Accurate determination of the leachability of arsenic in the waste is crucial for both economic concerns and the evaluation of environmental impacts.

The disposal of solid wastes is regulated by the U.S. EPA and state agencies according to the leaching potential of pollutants determined by standard extraction tests. The Toxicity Characteristic Leaching Procedure (TCLP) is the current U.S. EPA standard protocol to identify hazardous materials, although its limitations have been recognized (*4*−*6*). A waste is deemed as hazardous material if the arsenic concentration in the TCLP leachate exceeds 5 mg L^{-1}. The Waste Extraction Test (WET) is a more aggressive leaching test adopted by the State of California with a regulatory concentration of 5 mg L^{-1}.

Arsenic adsorption and removal from source water has been extensively investigated in the past decades; however, few studies have attempted to evaluate the arsenic leachability from spent adsorbent media. The As leaching potential in water treatment residues is strongly related to the redox potential and arsenic species (*5*, *7*). The low As leachability in water treatment sludge was attributed to the high affinity of the iron oxides and alumina surfaces for As (*8*, *9*). Desorption was one of the most important factors controlling As(V) mobilization from waste adsorbents (*6*). The dissolution of Fe and arsenic minerals was considered to be the major mechanism for naturally occurring arsenic in Bangladesh (*10*).

Arsenic adsorption onto metal oxides has been extensively investigated with extended X-ray absorption fine structure (EXAFS) spectroscopy (*11*−*13*). Previous studies have shown that arsenate adsorbs onto iron oxides and alumina through the formation of inner-sphere surface complexes with a predominantly bidentate configuration, along with a minor monodentate contribution. These techniques have been successfully applied to study arsenic immobilization mechanisms in water treatment sludge (*7*, *9*).

In the present study, arsenate leachability in five spent media was evaluated with the TCLP, WET and desorption tests. The local coordination environment of arsenate on the media was investigated with EXAFS. This study improved the understanding of the leaching behaviors of arsenic in the spent media and its relation to the As local coordinate structure.

Materials and Methods

Adsorbents. The spent adsorbents were collected from the pilot-scale filters used for treatment of arsenic in groundwater at Hopewell, NJ. The adsorption columns, containing GFH (US Filter, Iowa), GFO (Apyron Technologies, Georgia), TiO$_2$ (Hydroglobe, New Jersey), AA (Alcan, Ohio), and MAA (Alcan, Ohio), were operated in parallel at the wellhead. Three liters of adsorbents was packed in a 3.785-L (1-gallon) filter house with an inside diameter of 11.43 cm (4.5 in.). The groundwater was continuously passed through the filter at an empty bed contact time (EBCT) of 3 min. Raw water As was in the As(V) form, and its concentration varied in the range of 39−53 μg L^{-1} (*14*). When the effluent As concentration was higher than the breakthrough concentration of 10 μg L^{-1}, the filtration treatment was stopped. The mass of the As retained in an adsorbent was calculated on the basis of the total volume of water filtered and arsenic concentrations in the influent and effluent.

The granular TiO$_2$ was made of nanocrystalline anatase that was developed by Meng et al. (*15*). The particle size of the granular TiO$_2$ was between 30 and 60 U.S. standard mesh (0.6−0.25 mm), and the specific surface area was ~180 m^2 g^{-1}. The Ti−OH site density is 2.7 mmol g^{-1} with total pore volume of 0.207 cm^3 g^{-1}. GFH and GFO were iron-based adsorbents made from akaganéite and goethite, respectively.

---

* Corresponding author phone: (201) 216-8994; fax: (201) 216-8303; e-mail: cjing@stevens.edu.

† Stevens Institute of Technology.

‡ New Jersey Department of Environmental Protection.

10.1021/es050290p CCC: $30.25

TABLE 1. Composition of the Spent Media

			metal content obtained from acid digestion, mg kg^{-1}							
medium	pH	water content %	As calcd[a]	As exptl[b]	Al	Ca	Fe	Mg	Mn	Ti
GFH	7.62	46.5 ± 0.2	2420	2240 ± 130	419 ± 19	7039 ± 122	674 600 ± 9377	506 ± 4	659 ± 7	69 ± 6
GFO	7.97	52.0 ± 0.2	5660	5840 ± 40	28 ± 1	2883 ± 66	617 200 ± 19 760	699 ± 1	1610 ± 10	48 ± 1
TiO_2	7.62	50.3 ± 0.5	3554	13 ± 2	44 ± 2	14 480 ± 701	428 ± 33	1300 ± 131	63 ± 6	1532 ± 255
AA	8.02	35.3 ± 0.5	226	194 ± 30	472 000 ± 10 900	3710 ± 9	57 ± 10	570 ± 11	ND[c]	25 ± 7
MAA	7.74	31.6 ± 0.1	443	412 ± 54	448 000 ± 2440	3257 ± 11	23 350 ± 324	398 ± 3	49 ± 1	63 ± 14

[a] Calculated results based on mass balance. [b] Acid digestion analysis results. [c] Not detectable.

The grain size was 30−60 mesh for GFO and 0.32−2.0 mm for GFH. AA and MAA were made of activated alumina and iron-impregnated AA, respectively. The grain size of AA and MAA was 28−48 mesh.

Acid Digestion. Triplicate samples of dried spent adsorbents (1.00 g) were digested using 1:1 HNO_3, concentrated HNO_3, and 30% H_2O_2 repeatedly at 95 °C on a hotplate (*16*). After cooling, the digested samples were diluted to 100 mL with DI water for analysis of metal content. The arsenic concentration was analyzed by Zeeman graphite furnace atomic absorption spectrometry (AAS) with a method detection limit (MDL) of 0.7 μg L^{-1}. The concentration of Al, Ca, Fe, Mg, Mn, and Ti was determined by inductively coupled plasma (ICP) emission spectrometry with MDLs of 30, 9, 7, 20, 8, and 6 μg L^{-1}, respectively.

Leaching Tests. The TCLP and WET were used to evaluate the leaching potential of arsenic in spent adsorbents. Triplicate samples were tested, and the mean value and standard deviation were calculated.

The TCLP test was conducted according to U.S. EPA protocol (*17*) by mixing 5 g of adsorbent samples with an extraction solution at a liquid to solid (L/S) ratio of 20. The extraction solution consisted of 0.1 M acetic acid and 0.0643 M NaOH with a pH of 4.93. The solid and leachant suspension was placed in a capped polypropylene bottle and tumbled at 30 rpm for 18 h. After extraction, the final pH of the leachate was measured, and the liquid was separated by filtration through a 0.45-μm glass fiber filter. The soluble arsenic concentration in the filtrate was analyzed with AAS.

The California WET (*18*) was conducted by mixing the solid sample with 0.2 M citrate buffer solution at pH 5 with a L/S ratio of 10 for 48 h. Before the extraction, the suspension was purged with N_2 for 15 min to expel the dissolved oxygen (DO).

Desorption Tests. Batch desorption experiments were conducted to determine the arsenic leaching potential in a 0.04 M NaCl solution at L/S ratio of 20. Fifteen suspension samples were prepared for each spent adsorbent and were adjusted to desired pH values in the range of 3−11 with HCl and NaOH. After 24 h of tumbling at 30 rpm in the dark, the equilibrium pH was measured, and the suspension was filtered through a 0.4-μm glass fiber filter. The soluble arsenic concentration in the filtrate was analyzed with AAS.

Surface Complexation Modeling. The charge distribution multisite complexation (CD-MUSIC) model with the triple plane option was used to describe desorption experimental data. The basic principles of the model have been well-documented in the literature (*19*−*21*). In the CD-MUSIC model, the oxygens on the surface are divided into singly (SO), doubly (S_2O), and triply (S_3O) coordinated groups to account for the different types of sites. The charge of the surface oxygen is affected by the adsorption of protons and the positive charge of metal ions present in the solid. Application of Pauling's bond valence concept leads to the definition of surface groups and their corresponding charge.

Singly coordinated surface hydroxyl groups can form inner-sphere complexes with As(V) (*19*−*21*). The charge of the adsorbed arsenic is spatially distributed over two electrostatic planes. The first plane (0-plane) contains the surface groups with the oxygens shared between the surface and arsenic. The second plane (1-plane) holds the solution oriented oxygen groups of the adsorbed arsenic. The outermost plane (2-plane) is the head end of the Gouy−Chapman diffuse double layer (DDL). The inner capacitance (C_1) is 2.36 F m^{-2} for TiO_2 (*21*), and 1.1 F m^{-2} for aluminum and iron (hydr)oxides (*20, 22*). The outer capacitance (C_2) is set to 5 F m^{-2}, as for most oxides (*19*). The calculation was performed using the chemical equilibrium program Visual MINTEQ (*23*) with the 1-pk TPM adsorption option.

EXAFS Analysis. The spent adsorptive media samples were sealed between two layers of Kapton tape. The spectra were collected on beamline X19A at the National Synchrotron Light Source (NSLS) in Brookhaven National Laboratory. An energy range of −200 to 1000 eV from the K-edge of As (11 868 eV) was used to acquire the spectra at room temperature. All spectra were collected in fluorescence mode using a passivated implanted planar silicon (PIPS) detector. An average of four scans was collected to achieve an adequate signal/noise ratio. Standard reference arsenic chemicals, $NaAsO_2$ and $Na_2HAsO_4 \cdot 7H_2O$, were also analyzed. Elemental arsenic (As^0) was used to calibrate the energy at 11 868 eV.

The EXAFS spectra were analyzed with the Athena and Artemis program of the IFEFFIT computer package (*24*). The spectra were processed by removing the background absorbance with a linear function through the pre-edge region, normalizing the atomic absorption, and extracting the EXAFS signal from the spectra. The spectra were converted to frequency (k) space and weighted by k^3, generating $k^3\chi(k)$ spectra. $k^3\chi(k)$ in k-space (Å^{-1}) was Fourier transformed (FT) to produce the radial structure function (RSF) in R-space (Å). The experimental spectra were fitted with single-scattering theoretical phase-shift and amplitude functions calculated with the ab initio computer code FEFF6 (*25*) using atomic clusters generated from the crystal structure of scorodite ($FeAsO_4 \cdot 2H_2O$). For Al- and TiO_2-based adsorbents, theoretical phase-shift and amplitude functions for a hypothetical cluster of atoms were generated by replacing the Fe atom in scorodite with Al and Ti, respectively. The many-body amplitude reduction factor (S_0^2) was fixed at 0.9. Each spectrum was fit by first isolating and fitting the first-shell As−O to estimate ΔE_0, the difference in threshold energy between theory and experiment, by fixing coordination numbers (CN) at 4 and Debye−Waller parameter (σ^2) at 0. Then ΔE_0 was fixed to the best fit value from first-shell fitting. The CN of As−O and As−Fe was initially fixed at 4 and 2, respectively, to obtain estimated values for interatomic distances (R) and σ^2. Finally, the spectrum was fitted using estimated values for CN, R, and σ^2 as starting values. Error estimates of the fitted parameters were CN, ±20%; R, ±0.02 Å; and σ^2, ±20−30%.

Results and Discussion

Spent Media. The physical and chemical properties of the waste adsorbent samples are summarized in Table 1. The mean value and the standard deviation of triplicate samples are reported. The pH of waste adsorbents ranged from 7.62 to 8.02. The water content varied from 31.6 to 52.0%. The arsenic content in spent media was determined by the total acid digestion method (*16*), and the mass balance calculation was based on the amount of arsenic removed from the water. Total As contents determined with the two methods were similar for all the spent media except for the TiO_2 sample. The As content determined with the acid digestion method (13 mg kg^{-1}) was 2 orders of magnitude less than the calculated content (3554 mg kg^{-1}). This was because only ~1.5 g Ti/kg TiO_2 was dissolved with the acid digestion (Table 1).

The total arsenic content varied from 226 to 5660 mg kg^{-1} of dry solids in the spent media. The amount of arsenic in the spent media was in the sequence of AA < MAA < GFH < TiO_2 < GFO. The As content in the widely used aluminum-based adsorbents (AA and MAA) was an order of magnitude less than that in the Fe- and Ti-based adsorbents (GFH, GFO, and TiO_2). This demonstrated that Al-based adsorbents are less effective for As adsorption than the other three media. The As content in MAA (412 mg kg^{-1}) was approximately double that in AA (194 mg kg^{-1}). This might be attributed to the addition of Fe in MAA, which enhanced the media adsorption capacity.

EXAFS Studies. EXAFS spectroscopy was employed to determine the arsenic local coordination environment of the waste adsorbent media. The k^3-weighted As K-edge EXAFS spectra are shown in Figure 1A, and the corresponding radial structure functions (RSF) are shown in Figure 1B as Fourier transformation (FT) vs radial distance for the spent media. The optimal parameters listed in Table 2 were obtained by fitting the theoretical curves to the experimental spectra. The FT of EXAFS spectra can isolate the contributions of different coordination shells, in which the peak positions correspond to the interatomic distances; however, these peak positions are uncorrected for phase shift so that they are shifted from the true distance by 0.3−0.5 Å.

Based on the fit of the theoretical to the experimental spectra, the first and strongest peak in the FT curve was contributed by four oxygen atoms at an average distance of 1.69 Å for all five media samples (Table 2). The constant As−O interatomic distance was independent of the media to which the As(V) was adsorbed. This suggested the AsO_4 tetrahedral geometry remained relatively rigid on the media surfaces.

The FT curves for all samples displayed distinct second peaks at an average interatomic distance of 3.13−3.32 Å (Figure 1B). This second shell can be fitted with 2 and 2.5 Fe atoms at 3.32 and 3.28 Å for GFO and GFH, respectively. The distances and coordination numbers (CN) of As−O and As−Fe are in good agreement with previously published data (*11*, *13*, *26*). Quantitative EXAFS fitting results for TiO_2 show the presence of a Ti atom with a CN of 2.1 at 3.27 Å. For AA and MAA, an average CN of 2.3 and 2.1 Al atoms were responsible for the second peak at 3.14 and 3.13 Å, respectively. Similar As−Al distances of 3.11 Å (*27*) and 3.19 Å (*12*) were previously reported. The second shell interatomic distance increased in the sequence of As−Al, As−Ti, and As−Fe, which was consistent with the slightly greater ionic radius succession of Al(III) (0.68 Å), Ti(IV) (0.75 Å), and Fe(III) (0.79 Å) (*28*).

The EXAFS results show that As(V) formed bidentate binuclear inner-sphere complexes on the surfaces of these five spent adsorbents. The findings of the As(V) surface structure are consistent with previous reports of the association of As(V) with iron and aluminum oxides (*11*−*13*, *26*, *27*). This stable structure is also observed for an As(V)−MnO_2 complex (*29*). The ab initio quantum mechanic calculation demonstrates this bidentate binuclear corner sharing geometry has the lowest total energy of the system (*12*, *13*, *29*). This stable structure can be used to explain the high affinity of As(V) for the adsorbent surfaces.

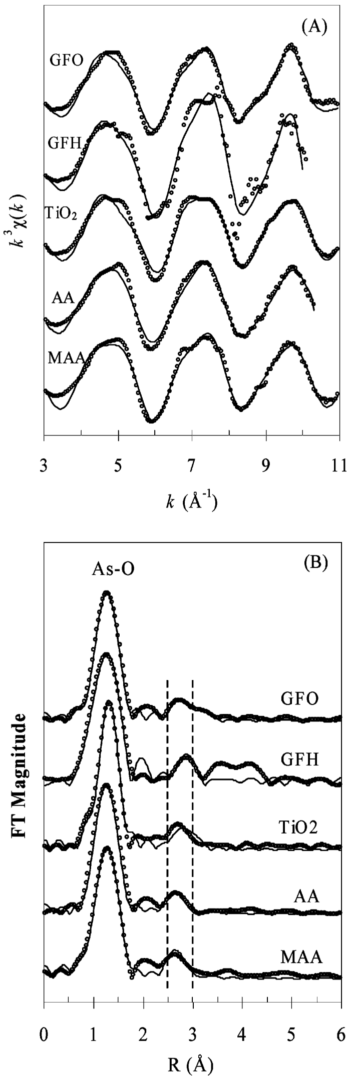

FIGURE 1. The k^3 weighted observed (dotted line) and model calculated (solid line) As K-edge EXAFS spectra (A) and Fourier transform magnitude (B) resulting in a radial distance structure for the spent media. The peak positions are uncorrected for phase shift. Arsenic formed binuclear bidentate surface complexes on the media surface.

TABLE 2. Local Coordination Environment of As in the Spent Media Determined by EXAFS

medium	shell	CN[a]	R(Å)[b]	σ^2[c]
GFO	As−O	4.1 ± 0.4	1.70 ± 0.01	0.0013 ± 0.0009
	As−Fe	2.0 ± 0.8	3.32 ± 0.03	0.0058 ± 0.0040
GFH	As−O	3.6 ± 0.3	1.68 ± 0.01	0.0030 ± 0.0011
	As−Fe	2.5 ± 1.0	3.28 ± 0.04	0.0052 ± 0.0012
TiO_2	As−O	4.2 ± 0.2	1.69 ± 0.01	0.0014 ± 0.0004
	As−Ti	2.1 ± 0.7	3.27 ± 0.02	0.0060 ± 0.0027
AA	As−O	4.3 ± 0.5	1.69 ± 0.01	0.0016 ± 0.0011
	As−Al	2.3 ± 1.4	3.14 ± 0.06	0.0049 ± 0.0074
MAA	As−O	4.1 ± 0.3	1.70 ± 0.01	0.0009 ± 0.0006
	As−Al	2.1 ± 0.6	3.13 ± 0.03	0.0078 ± 0.0030

[a] Coordination number. [b] Interatomic distance. [c] Debye−Waller parameter.

To further understand the EXAFS information and identify the As neighboring atoms, the continuous cauchy wavelet transform (CCWT) was performed. The details of the theory

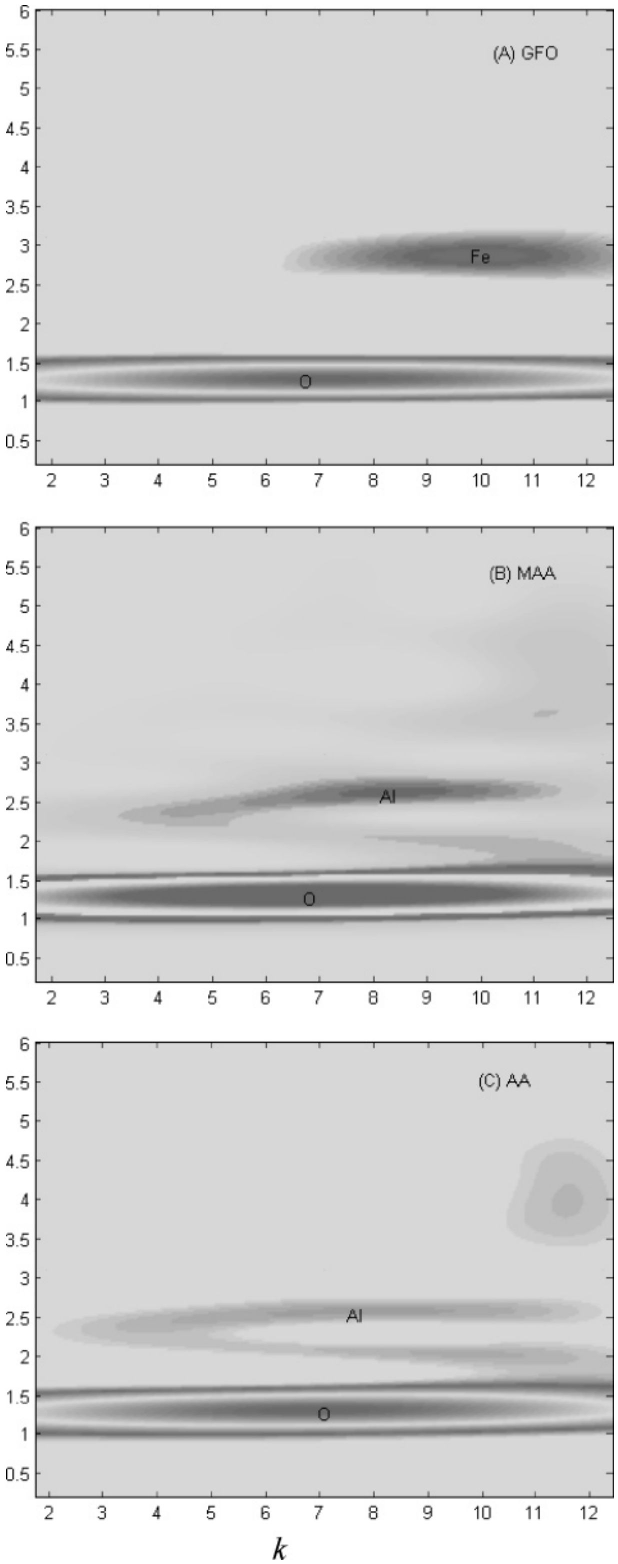

FIGURE 2. CCWT analysis of a two-dimensional EXAFS decomposition in *k*-space (wave vector) and R-space (phase-uncorrected distance) for GFO (A), MAA (B), and AA (C).

and application in EXAFS analysis were reported by Muñoz et al. (*30*). The CCWT results in Figure 2 show a two-dimensional EXAFS decomposition in *k* space (wavevector) and R space (phase uncorrected distance). Two distinct ridges were found in the CCWT modulus, corresponding to the two atoms neighboring the center As. On the basis of the previous EXAFS analysis, the oxygen was the first As neighboring atom that centered at ~7 Å^{-1} in *k* space for GFO, MAA, and AA samples (Figure 2). A second neighbor contribution in GFO sample was an Fe atom, which was centered at ~10 Å^{-1}. The Fe atom resulted in a higher value in *k* space than the O atom. An atom with high *Z* (atomic number) is more efficiently backscattered at high *k* value, compared with low-*Z* atoms, which are backscattered at low *k* value (*30*). The second shell of MAA and AA centered at ~8.5 Å^{-1}, suggesting the presence of the same Al atom in this coordination shell. Furthermore, the lower *Z* value of the Al atom was demonstrated by its lower *k* value than that of the Fe atom.

The Al_2O_3 content was more than 85% in the spent MAA sample, and Fe_2O_3 only contributed to <4% of total weight (Table 1). Although some As may be associated with Fe in the spent MAA, the contribution of As−O−Fe complexes to the EXAFS signal may be outweighed by the majority of As−O−Al complexes.

Desorption. Desorption tests were employed to simulate the arsenic leaching potential from the spent adsorbents. The results in Figure 3 show the release of arsenic from the spent media as a function of final solution pH. The release of arsenic had a minimum in a pH range between 5 and 7 and increased dramatically when pH increased from 7 to 11. Solution arsenic concentrations were less than 10 μg L^{-1} in all spent medium suspensions at pH 5−7 (Figure 3A). When pH > 7, soluble As concentrations in AA, MAA, and GFH were in the same order of magnitude, which were 10 times lower than that of GFO and TiO_2. This could be attributed to a higher arsenic content in the spent GFO and TiO_2 than in the other adsorbents. The extractable As concentration reached as high as 7610 μg L^{-1} at pH 11 for the GFO sample. This observation is in good agreement with the anion adsorption characteristic of As(V) in water treatment residues (*7*, *9*).

In the present study, the bidentate binuclear arsenic complexes determined with EXAFS were incorporated into the CD-MUSIC model to describe As(V) desorption from the spent media. The CD-MUSIC model has been employed to describe the adsorption behaviors of iron oxides (*19*, *20*), aluminum oxides (*22*), and TiO_2 (*21*). The surface acid−base reactions, formation of outer-sphere complexes with background electrolytes, and their corresponding adsorption constants were obtained from references and listed in Table 3. Only singly coordinated surface groups were responsible for the arsenic adsorption in the CD-MUSIC modeling. The charge distribution (CD) value expressed the fraction *f* of the charge of the central As ion attributed to the surface plane, and the remaining part (1 − *f*) was attributed to the other ligands of the complex, which were located in the 1-plane. The assumption for the CD factor *f* was based on the theoretical value from the Pauling rule of equal distribution over the surrounding ligands. For bidentate As surface complexes, two ligands were placed in the 0-plane. Thus, *f* was set to 0.5 (2/4) since As(V) has four ligands. The only adjustable parameter is the formation constant of the inner-sphere As complexes. The optimized adsorption constant of the $S_2O_2AsO_2$ complex was in the range of 24.8 to 27.2, obtained by fitting desorption experimental data for each media.

According to the arsenic and water content in the media (Table 1) and the liquid-to-solid ratio of 20 used in the extraction, the total arsenic and adsorbent concentrations in the desorption experiment were calculated and are presented in Table 3. A fixed ionic strength of 0.04 M was used in the model calculations by entering 0.04 M NaCl as background electrolyte. The results of the model calculation in Figure 3 showed that the bidentate As(V) surface complex model fitted well the arsenic concentrations in the extraction system. The model underestimated the As concentrations at pH < 7 for GFO, GFH, AA, and MAA. This might be ascribed to the dissolution of the media at low pH.

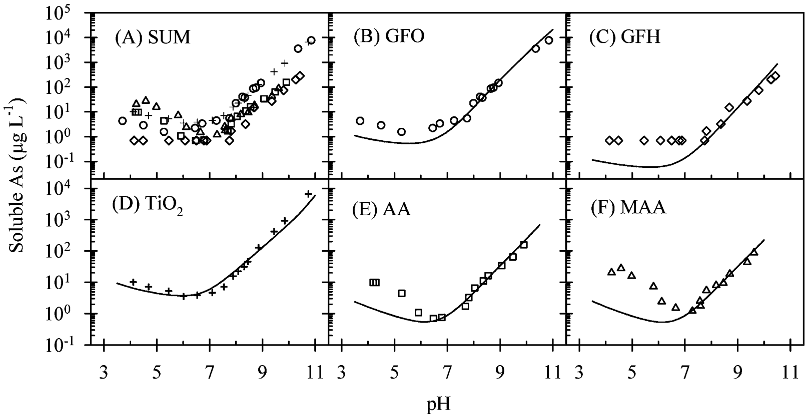

FIGURE 3. Release of As in 0.04 M NaCl extraction solution for all spent adsorbents (A), and CD-MUSIC modeling results for GFO (B), GFH (C), TiO$_2$ (D), AA (E), and MAA (F) samples.

TABLE 3. Surface Parameters and Species Used in the CD-MUSIC Modeling

											log K				
species	P_0[a,d]	P_1[b,d]	P_2[c,d]	SOH	S_2O	S_3O	H	AsO_4	Na	Cl	GFH	GFO	TiO_2	AA	MAA
$SOH^{-1/2}$				1											
$SOH_2^{+1/2}$	1			1			1				9.2^e	9.2^e		9^f	9^f
$SOHNa^{+1/2}$			1	1					1		0.2^f	0.2^f		0.2^f	0.2^f
$SOH_2Cl^{-1/2}$	1		−1	1			1			1	9^e	9^e		8.8^f	8.8^f
$S_3O^{-1/2}$						1									
$S_3OH^{+1/2}$	1					1	1				9.2^e	9.2^e		7^f	7^f
$S_3ONa^{+1/2}$			1			1			1		0.2^f	0.2^f		0.2^f	0.2^f
$S_3OHCl^{-1/2}$	1		−1			1	1			1	9^e	9^e		6.8^f	6.8^f
$S_2O_2AsO_2^{-2}$	0.5	−1.5		2			2	1			26.5^g	27.2^g		26.3^g	26.9^g
$TiOH^{-1/3}$				1											
$TiOH_2^{+2/3}$	1			1			1						5.8^h		
$TiOHNa^{+2/3}$			1	1					1				-0.6^i		
$TiOH_2Cl^{-1/3}$	1		−1	1			1			1			4.7^i		
$Ti_2O^{-2/3}$					1										
$Ti_2OH^{+1/3}$	1				1		1						5.8^h		
$Ti_2ONa^{+1/3}$			1		1				1				-0.6^i		
$Ti_2OHCl^{-2/3}$	1				1		1			1			4.7^i		
$Ti_2O_2AsO_2^{-5/3}$	0.5	−0.5		2			2	1					24.8^g		
							Surface Site Density (nm^{-2})								
SOH											3.45^e	3.45^e	9.0^k	2.5^f	2.5^f
S_2O													9.0^k		
S_3O											2.7^e	2.7^e		2.5^f	2.5^f
surface area (m^2 g^{-1})											290^j	140^j	180^k	350^l	240^j
inner-sphere capacitance, C_1 (F m^{-2})											1.1^e	1.1^e	2.36^i	1.1^f	1.1^f
outer-sphere capacitance, C_2 (F m^{-2})											5^e	5^e	5^i	5^f	5^f
total As concn (mM)											0.800	1.871	1.179	0.084	0.188
adsorbent concn (g L^{-1})											26.8	24.0	24.9	32.4	34.2

[a] $P_0 = \exp(-F\Psi_0/RT)$. [b] $P_1 = \exp(-F\Psi_1/RT)$. [c] $P_2 = \exp(-F\Psi_2/RT)$. [d] Ψ_0, Ψ_1, Ψ_2 are the electrostatic potential (V) of 0-, 1-, and 2-plane, respectively; F = Faraday constant (C mol^{-1}); R = gas constant (J mol^{-1} K^{-1}); and T = absolute temperature (K). [e] From Hiemstra and Van Riemsdijk (*19–20*). [f] From Hiemstra et al. (*22*). [g] Best fit value. [h] From Jing et al. (*32*). [i] From Bourikas (*21*). [j] From Lytle et al. (*33*). [k] From Meng et al. (*15*). [l] From Alcan AA manufacturer.

TABLE 4. TCLP (0.1 M Acetate Solution) Results of the Spent Media

medium	pH	As (μg L^{-1})	Al (mg L^{-1})	Ca (mg L^{-1})	Fe (mg L^{-1})	Mg (mg L^{-1})	Mn (mg L^{-1})	Ti (mg L^{-1})
GFH	5.31 ± 0.01	ND	ND	162 ± 2	0.49 ± 0.09	10.7 ± 0.1	ND	ND
GFO	5.04 ± 0.02	ND	ND	52.9 ± 0.5	0.42 ± 0.06	11.4 ± 0.1	ND	ND
TiO_2	5.46 ± 0.02	180 ± 28	ND	317 ± 15	ND	14.2 ± 0.1	0.12 ± 0.04	ND
AA	5.22 ± 0.01	3.5 ± 0.2	19.2 ± 0.7	108 ± 1	ND	10.3 ± 0.1	ND	ND
MAA	5.16 ± 0.01	4.3 ± 0.2	94.8 ± 1.8	99.4 ± 9.8	0.23 ± 0.02	8.69 ± 0.06	ND	ND

Leachability. The TCLP and WET were used to evaluate the As leachability in spent media. The extraction was performed on triplicate samples for each adsorbent, and results of the TCLP and WET are shown in Tables 4 and 5, respectively. The leachate As speciation, as measured with high performance liquid chromatography/atomic fluorescence spectrometry (HPLC/AFS), confirmed that all extractable As was in the As(V) form (data not shown). The As concentration in the TCLP leachate was <5 μg L^{-1} for all spent media except the TiO$_2$ sample (Table 4). The average leachate As concentration of the TiO$_2$ sample was 180 μg L^{-1}, which is much lower than the TCLP regulatory 5 mg L^{-1}. The result was in agreement with previous conclusions that wastes generated in the treatment of source water were not

TABLE 5. WET (0.2 M Citrate Solution) Results of the Spent Media

medium	pH	As (μg L^{-1})	Al (mg L^{-1})	Ca (mg L^{-1})	Fe (mg L^{-1})	Mg (mg L^{-1})	Mn (mg L^{-1})	Ti (mg L^{-1})
GFH	5.47 ± 0.02	6650 ± 295	2.72 ± 0.69	355 ± 24	1880 ± 157	30.7 ± 0.4	4.32 ± 0.25	0.55 ± 0.27
GFO	5.04 ± 0.01	2460 ± 136	0.38 ± 0.05	88.9 ± 0.9	69.5 ± 1.0	35.6 ± 0.1	3.01 ± 0.14	0.40 ± 0.22
TiO_2	5.17 ± 0.01	2470 ± 280	0.44 ± 0.02	678 ± 52	1.06 ± 0.08	48.9 ± 0.7	0.61 ± 0.07	16.9 ± 2.2
AA	5.39 ± 0.01	282 ± 27	614 ± 28	173 ± 6	0.08 ± 0.02	31.9 ± 1.0	ND	0.12 ± 0.01
MAA	5.42 ± 0.01	308 ± 18	548 ± 46	207 ± 27	53.1 ± 0.9	24.8 ± 0.5	0.21 ± 0.01	0.45 ± 0.08

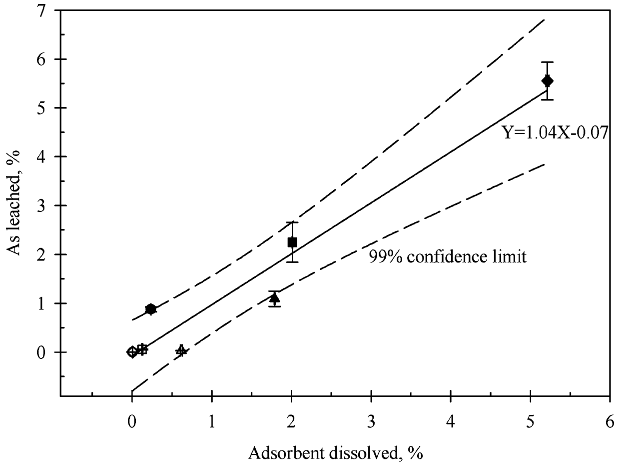

FIGURE 4. Correlation of percentage of As leached and adsorbent dissolution in GFH (◆, ◇), GFO (●, ○), AA (■, □), and MAA (▲, △) for the WET (closed), and TCLP (open), respectively. The solid line is the regression and the dashed lines are 99% confidence limits.

hazardous material according to the TCLP leachability (*7*–*9*).

Arsenic leachability determined with the WET extraction was much higher than that determined with the TCLP (Table 5). The As concentration varied from 282 to 6650 μg L^{-1} in the WET leachate. The leachate arsenic concentration for spent GFH was 6650 μg L^{-1}, which exceeded the WET limit of 5000 μg L^{-1}. The WET concentration for GFH is much higher than a recent report (*6*), which shows an As concentration <1 mg L^{-1} for a spent GFH. The discrepancy in the leaching results may be explained by the source of the spent GFH. Ghost et al. (*6*) used spent GFH prepared in a laboratory batch adsorption experiment.

The difference in the leachate As concentrations determined with WET, TCLP, and the desorption test could be attributed to different acids used in the leaching solutions. The As leachate concentrations were similar in TCLP and the desorption test at pH 5 (Table 4 and Figure 3). This observation is in agreement with the conclusion of Ghost et al. (*6*) that desorption is the most important factor controlling the As mobilization from the spent adsorbents determined with TCLP. Citric acid in the WET leachant is a stronger complexing agent than acetic acid in the TCLP leachant (*4*, *31*). Citrate may promote the Fe oxide dissolution, which induces the As(V) release (*7*). In addition, more adsorbent was dissolved in the WET leachate than that in the TCLP, although the final leachate pH values were similar in both tests (Tables 4, 5). The correlation of the percentage of As leached with the percentage of the adsorbent dissolved for the media is shown in Figure 4. The correlation coefficient of the linear regression was 1.04 with $R^2 = 0.95$. The dashed lines in Figure 3 show the 99% confidence limits. The amount of As released was positively related to the amount of adsorbent dissolved in the leachate, which suggests that adsorbent dissolution may be the main mechanism of enhanced As release in the WET.

Environmental Impact. With the prevailing usage of adsorption processes in the point-of-entry/point-of-use (POE/POU) for the As removal, proper disposal of spent media containing elevated arsenic content is a critical issue. To predict the fate and transport of As in the wastes, it is essential to understand As retention/leaching mechanisms. The As adsorption mechanism determined with EXAFS was the formation of inner-sphere bidentate binuclear surface complexes on the adsorbent surfaces. The adsorption/desorption behavior can be successfully formulated and predicted with the CD-MUSIC model for each media. The amount of As released was positively related to the amount of adsorbent dissolved in the leachate, which suggests that adsorbent dissolution may be the main mechanism for As release. An aggressive chelating agent, such as citric acid, could form soluble complexes with the adsorbent and release the arsenic. This is especially important for the GFH, which failed in the WET. A moderate organic acid, such as acetic acid, could only extract arsenic at a low concentration, <180 μg L^{-1}. However, this kind of organic acid is a relatively stable degradation product of organic matter and is widely available in landfill leachate. Thus, codisposal of arsenic containing wastes with municipal solid waste (MSW) may have a potential risk of arsenic recontamination. With the higher As adsorptive capacity, GFO and TiO_2 were better adsorptive media in As removal than GFH, AA, and MAA. In addition, TCLP and WET results indicated that the two spent media were nonhazardous material.

Acknowledgments

We acknowledge the staff on beamline X19A at the National Synchrotron Light Source (NSLS) for their assistance with EXAFS analysis.

Literature Cited

(1) Christen, C. New Jersey proposes toughest arsenic standard worldwide. *Environ. Sci. Technol.* **2004**, *38*, 105A.

(2) Driehaus, W.; Jekel, M.; Hildebrandt, U. Granular ferric hydroxide—a new adsorbent for the removal of arsenic from natural water. *J. Water SRT-Aqua* **1998**, *47*, 30–35.

(3) U.S. EPA. Arsenic treatment technology evaluation handbook for small systems. EPA-816-R-03-014; U.S. Government Printing Office: Washington, DC, 2003.

(4) Hooper, K.; Iskander, M.; Sivia, G.; Hussein, F.; Hsu, J.; Deguzman, M.; Odion, Z.; Ilejay, Z.; Sy, F.; Petreas, M.; Simmons, B. Toxicity characteristic leaching procedure fails to extract oxoanion-forming elements that are extracted by municipal solid waste leachates. *Environ. Sci. Technol.* **1998**, *32*, 3825–3830.

(5) Meng, X.; Korfiatis, G. P.; Jing, C.; Christodoulatos, C. Redox transformations of arsenic and iron in water treatment sludge during aging and TCLP extraction. *Environ. Sci. Technol.* **2001**, *35*, 3476–3481.

(6) Ghost, A.; Mukiibi, M.; Ela, W. TCLP underestimates leaching of arsenic from solid residuals under landfill conditions. *Environ. Sci. Technol.* **2004**, *38*, 4677–4682.

(7) Jing, C.; Liu, S.; Meng, X. Arsenic leachability and speciation in cement immobilized water treatment sludge. *Chemosphere* **2005**, *59*, 1241–1247.

(8) U.S. EPA. Treatment of arsenic residuals from drinking water removal processes. EPA-600-R-01-033; U.S. government Printing Office: Washington, DC, 2001.

(9) Jing, C.; Korfiatis, G. P.; Meng, X. Immobilization mechanisms of arsenate in iron hydroxide sludge stabilized with cement. *Environ. Sci. Technol.* **2003**, *37*, 5050–5056.

(10) Nickson, R.; McArthur, J.; Burgess, W. G.; Ahmed, K. M.; Ravenscroft, P.; Rahman, M. Arsenic poisoning of Bangladesh groundwater. *Nature* **1998**, *395*, 338.

(11) Fendorf, S.; Eick, M. J.; Grossl, P.; Sparks, D. L. Arsenate and chromate retention mechanisms on goethite. 1. surface structure. *Environ. Sci. Technol.* **1997**, *31*, 315−320.

(12) Ladeira, A. C. Q.; Ciminelli, V. S. T.; Duarte, H. A.; Alves, M. C. M.; Ramos, A. Y. Mechanism of anion retention from EXAFS and density functional calculations: Arsenic(V) adsorbed on gibbsite. *Geochim. Cosmochim. Acta* **2001**, *65*, 1211−1217.

(13) Sherman, D. M.; Randall, S. R. Surface complexation of arsenic(V) to iron(III) (hydr)oxides: structural mechanism from ab initio molecular geometries and EXAFS spectroscopy. *Geochim. Cosmochim. Acta* **2003**, *67*, 4223−4230.

(14) Bang, S. B.; Patel, M.; Lippincott, L.; Meng, X. G. Removal of arsenic from groundwater by granular titanium dioxide adsorbent. *Chemosphere*, in press.

(15) Meng, X. G.; Dadachov, M.; Korfiatis, G. P.; Christodoulatos, C. Method of preparing a surface-activated titanium oxide product and of using the same in water treatment processes. U.S. Patent 20030155302, 2003.

(16) U.S. EPA. *Test Methods for Evaluating Solid Waste, Physical/Chemical Methods*, SW-846, 3rd ed.; Method 3050B; U.S. Government Priniting Office: Washington, DC, 1992.

(17) U.S. EPA. *Test Methods for Evaluating Solid Waste, Physical/Chemical Methods*, SW-846, 3rd ed.; Method 1311; U.S. Government Priniting Office: Washington, DC, 1992.

(18) California Code of Regulations (CCR). *California Waste Extraction Test*; Title 22, Division 30, California Register 85, no 2: 1800, 78-1800.82; 1985.

(19) Hiemstra, T.; Van Riemsdijk, W. H. A surface structural approach to ion adsorption: the charge distribution (CD) model. *J. Colloid Interface Sci.* **1996**, *179*, 488−508.

(20) Hiemstra, T.; Van Riemsdijk, W. H. Surface structural ion adsorption modeling of competitive binding of oxyanions by metal (hydr)oxides. *J. Colloid Interface Sci.* **1999**, *210*, 182−193.

(21) Bourikas, K.; Hiemstra, T.; Van Riemsdijk, W. H. Ion pair formation and primary charging behavior of titanium oxide (anatase and rutile). *Langmuir* **2001**, *17*, 749−756.

(22) Hiemstra, T.; Yong, H.; Van Riemsdijk, W. H. Interfacial charging phenomena of aluminum (Hydr)oxides. *Langmuir* **1999**, *15*, 5942−5955.

(23) Gustafsson, J. P. Modeling molybdate and tungstate adsorption to ferrihydrite. *Chem. Geol.* **2003**, *200*, 105−115.

(24) Newville, M. IFEFFIT: interactive XAFS analysis and FEFF fitting. *J. Synchrotron Rad.* **2001**, *8*, 322−324.

(25) Mustre de Leon, J.; Rehr, J. J.; Zabinsky, S. I.; Albers, R. C. Ab initio curved-wave X-ray absorption fine structure. *Phys. Rev. B* **1991**, *44*, 4146−4156.

(26) Waychunas, G. A.; Rea, B. A.; Fuller, C. C.; Davis, J. A. Surface chemistry of ferrihydrite. 1. EXAFS studies of the geometry of coprecipitated and adsorbed arsenate. *Geochim. Cosmochim. Acta* **1993**, *57*, 2251−2269.

(27) Arai, Y.; Elzinga, E. J.; Sparks, D. L. X-ray absorption spectroscopic investigation of arsenite and arsenate adsorption at the aluminum oxide-water interface. *J. Colloid Interface Sci.* **2001**, *235*, 80−88.

(28) Miessler, G. L.; Tarr, D. A. *Inorganic Chemistry*, 2nd ed.; Prentice Hall: New Jersey, 1999.

(29) Manning, B. A.; Fendorf, S. E.; Bostick, B.; Suarez, D. Arsenic(III) oxidation and arsenic(V) adsorption reactions on synthetic birnessite. *Environ. Sci. Technol.* **2002**, *36*, 976−981.

(30) Muñoz, M.; Argoul, P.; Farges, F. Continuous cauchy wavelet transform analyses of EXAFS spectra: a qualitative approach. *Am. Mineral.* **2003**, *88*, 694−700.

(31) Miller, W. P.; Zelazny, L. W.; Martens, D. C. Dissolution of synthetic crystalline and noncrystalline iron oxides by organic acids. *Geoderma* **1986**, *37*, 1−13.

(32) Jing, C.; Meng, X.; Liu, S.; Baidas, S.; Christodoulatos, C.; Korfiatis, G. P. Surface complexation of organic arsenic on nanocrystalline titanium oxide. *J. Colloid Interface Sci.*, in press.

(33) Lytle, D. A.; Payne, J. M.; Sorg, T. J. Adsorption media for arsenic removal. In *Workshop on the Design and Operation of Adsorptive Media Processes for the Removal of Arsenic from Drinking Water*, Cincinnati, OH, 2004.

Received for review February 11, 2005. Revised manuscript received April 26, 2005. Accepted May 4, 2005.

ES050290P